Appendix 2

Contents:

The NORSAR Regional Arrays

NORSAR operates the two regional seismic arrays, ARCES (near Karasjok, Finnmark) and SPITS (on Svalbard). In addition, data from NORSAR (the original large aperture array in southern Norway), FINES (in Finland), HAGFORS (southern Sweden), KBS (Kings Bay on Svalbard), KONO (Kongsberg, southern Norway), JMI (Jan Mayen) and APATITY (near Murmansk, Russia) are collected and analyzed.

Changes in the array instrumentation in 2003:

In June 2002 the NORES array was damaged by lightening. The damage was so comprehensive that a strategic decision on the future of NORES was needed. The array was not operating through 2003. The decision on how and when it will be reinstalled is still pending. We are presently investigating alternative processing and analysis algorithms that can be used with data from the large aperture NORSAR array. If successful this can compensate for the current lack of data from the NORES array. A short presentation of the status to this analysis improvements is provided below.

The HAGFORS (southern Sweden) array has been subject to a complete refurbishment. New sites have been constructed so that it is now a concentric 1+3+5 element array with a diameter of approximately 1.5 km. The sensors are one broad band and the other eight are short period instruments. The array center code HFS has been maintained, however, it now refers to a new point.

1 Systems Recording Performance

The arrays have continuous data recording. In 2003 the average recording time for the SPITS array was 99.4%, for the ARCES array 99.8%, and for the NORSAR array 100%.

The recording performance in terms of monthly uptime statistics is shown in Table 1.

	ARCES	SPITS	NORSAR
January	100 %	99.98 %	100 %
February	100 %	100 %	100 %
March	100 %	99.98 %	100 %
April	100 %	99.78 %	100 %
May	99.99 %	99.84 %	100 %
June	100 %	99.90 %	100 %
July	100 %	99.88 %	100 %
August	97.89 %	100 %	100 %
September	100 %	93.50 %	100 %
October	100 %	99.94 %	100 %
November	100 %	99.84 %	100 %
December	100 %	99.88 %	100 %

Table 1. Systems recording performance (uptime in % of theoretical) for three arrays operated by NORSAR in 2003.

2 Detections

The NORSAR analysis results are based on automatic phase detection and automatic phase associations which produce the automatic bulletin. Based on the automatic bulletin a manual analysis of the data is done, resulting in the reviewed bulletin (which is available under the NORSAR web pages). This procedure is often referred to as the Regional Monitoring System (RMS), and has been in operation since 1989. To reduce the work load on the analyst, the Generalized Beam Forming (GBF) is used as a pre-processor to RMS, so that only phases associated with selected events in northern Europe are considered in the automatic RMS phase association. However, all detections are available for analyst screening and review.

Table 2 gives a summary of the phase detections and events declared by the RMS.

	Jan.	Feb.	March	April	May	June
Phase detections	198714	140124	157067	156840	147444	170472
Associated phases	4891	4104	4717	4773	4674	5624
Un-associated phases	193823	136020	152350	152067	142770	164848
Events automatically declared by RMS	1086	874	965	974	846	1221
No. of events defined by the analyst	60	63	76	69	85	82
	July	Aug.	Sep.	October	Nov.	Dec.
Phase detections	192645	199361	184110	175425	158654	199536
Associated phases	5439	5951	7556	7043	6374	6346
Un-associated phases	187206	193410	176554	168382	152280	193190
Events automatically declared by RMS	1106	1372	1649	1504	1364	1445
No. of events defined by the analyst	113	43	73	46	91	72

Table 2. RMS phase detections and event summary.

2.1 NORSAR's Internet pages

NORSAR implemented new Internet pages in 2003 (www.norsar.no). The pages with bulletin information can now be found under the "Earthquake Reports" (http://www.norsar.no/NDC/bulletins/). Note that a Norwegian page "Norske jordskjelv" is also available under the Internet pages of NORSAR.

3 The use of Norwegian data

Data collected on Norwegian seismic stations are made available through the Internet and is provided on request to interested parties. The use and publication of this data is beyond our control. The published list below therefore only cover publications that we are aware of (mainly where one of us is a coauthor).

3.1 Processing of regional phases using the large aperture NOA array

This study has been undertaken to develop a substitute for the regional NORES array (which is currently in-operational) for inclusion in the NORSAR regional processing system. The NOA seismic array (originally called the NORSAR array) was designed to maximize signal coherence for teleseismic events and, at the same time, minimize the coherence of noise, therefore providing an optimal signal to noise ratio (SNR) for teleseismic phases using ordinary beamforming. With an inter-station separation of about 3 km, signal coherence is very low for seismic phases from regional events. In order to process regional phases using NOA, a special processing system is therefore required. We have developed such a system, which works by calculating the arrival times of phases at each of the short period vertical instruments in the array and by fitting a wavefront to those arrival times. The circular wavefront formulation of Almendros et al. (1999) was found to give very robust and realistic estimates of slowness and azimuth of phases at near-regional distances, an iterative process being employed to find the parameters which minimize time residuals. This iterative method could robustly be applied to all arriving wavefronts because the limiting case of the circular wavefront is a plane wavefront.

Automatic detections from the prototype regional NOA processing system have been included in a test version of the GBF process. The test version has been quite successful at locating events within approximately 350 km of the array and many events which have not been detected by the GBF system since the loss of the NORES array can now be included. The NOA array can also provide a useful constraint on events which otherwise would only be detected by the Hagfors array.

The remaining challenges to the process are to improve the determination of onset times for secondary phases and to improve the detection and processing of events at far-regional distances. The key to the first issue is almost certainly the use of the rotated horizontal components of the 3-component broadband instruments, of which one is located in each subarray. The key to the second issue is probably the use of detecting beams which cover more than one subarray: possibly with the additional use of the 3-component instruments.

We have in Attachment I included a paper prepared by S. J. Gibbons, T. Kværna and F. Ringdal entitled “Processing of regional phases using the large aperture NOA array”. This paper was published in the NORSAR Semiannual Report 2-2003, and is attached in its full length.

Attachment I

6.4 Processing of regional phases using the large aperture NOA array

6.4.1 Introduction

The NOA seismic array (originally called the NORSAR array) was conceived in the late 1960s for the detection of underground nuclear explosions at teleseismic distances. The array, completed in 1970, originally consisted of seismometers on 132 sites with a maximum spacing of over 100 km (Bungum et al., 1971, Bungum and Husebye, 1974). The array was arranged in the form of 22 subarrays, each containing 6 seismometer sites. NOA was designed to maximize signal coherence for teleseismic events and, at the same time, minimize the coherence of noise, therefore providing an optimal signal to noise ratio (SNR) for teleseismic phases using ordinary beamforming. In 1976, the array was reduced to the current configuration of 42 sites spread over 7 subarrays (Ringdal and Husebye, 1982). The configuration of the NOA array, past and present, is shown in Fig. 6.4.1.

It was, however, clear that with an inter-station separation of about 3 km, signal coherence was very low for seismic phases from regional events. In order to detect regional phases, a regional array with much smaller inter-station distances, NORES, was developed on the site of the 06C subarray of NOA (Mykkeltveit and Ringdal, 1981). The original 6-instrument experimental array was expanded to 25 instruments, arranged in four concentric rings, and was completed in 1984. This concept of regional seismic array has now been applied to many sites; e.g., GERES, ARCES, FINES, and SPITS have been based upon the NORES idea (see Mykkeltveit and Bungum, 1984; Mykkeltveit et al., 1990), FINES and SPITS having fewer sites.

The building housing the central processing systems for NORES was struck by lightning in June 2002, destroying all of the technical equipment inside. It is hoped that the array can be rebuilt, although technical and financial considerations mean that it is out of action for the foreseeable future. NORES was a key array in NORSAR's generalized beamforming (GBF) process which associates seismic phases from regional arrays and provides provisional, automatic locations for regional seismic events in the European Arctic (Ringdal and Kværna, 1989; Kværna and Ringdal, 1996). Until it is possible to rebuild NORES, or find an alternative regional array solution, it is highly desirable to try to use the NOA array for the detection and processing of regional events. This forms the motivation for the present study.

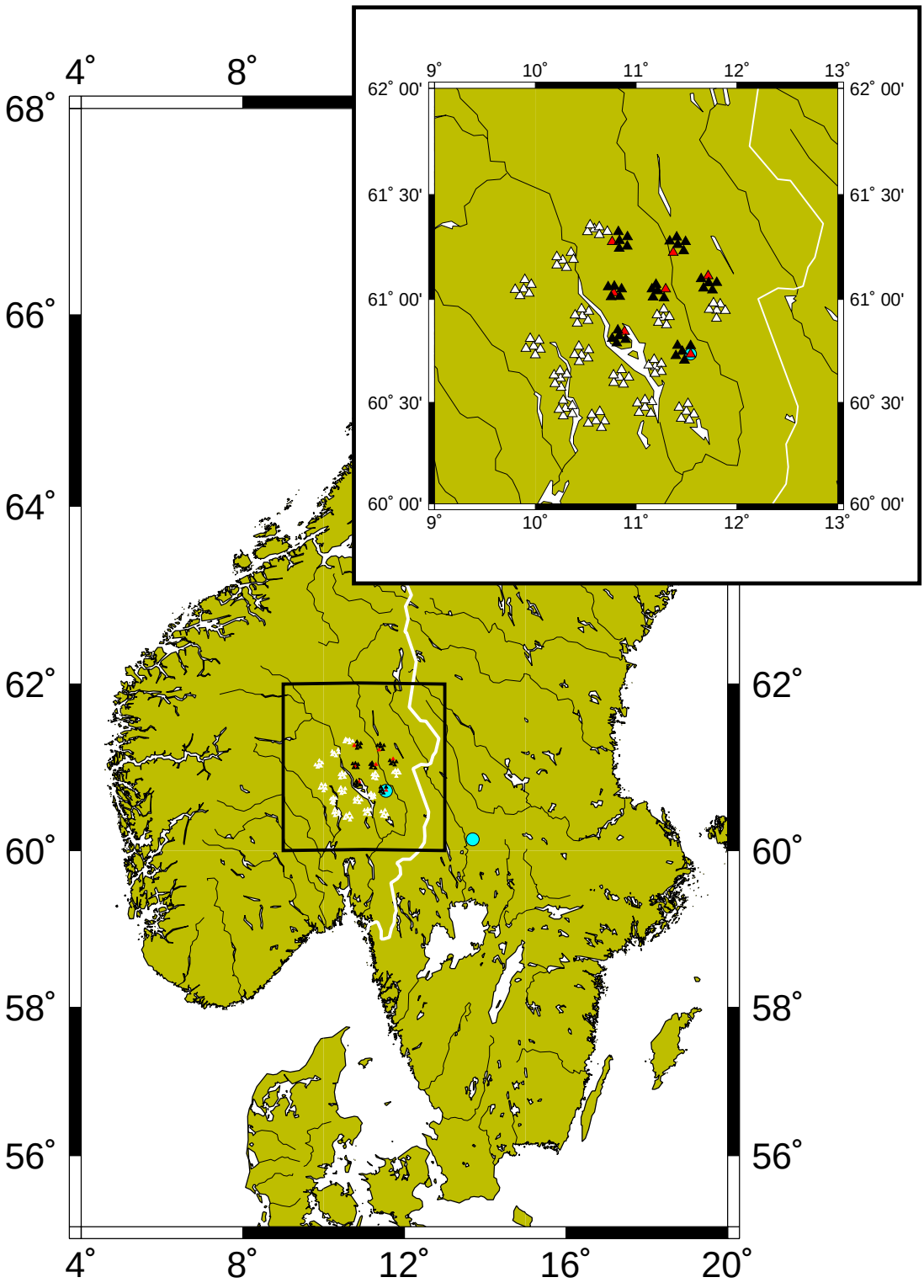

Fig. 6.4.1. The NOA seismic array. The inset diagram indicates the existing short period vertical stations as black triangles. Red triangles indicate that there is also a broadband 3-component instrument on the site and the white triangles are sites from the original array which were taken out of service in 1976. The blue circles represent the locations of the NORES and Hagfors regional arrays.

The large inter-station distances at NOA mean that traditional array techniques, such as broad-band fk-analysis, are only applicable to signals with a very low frequency content. This is illustrated by the cases in Fig. 6.4.2. Although both signals have a high SNR, only the teleseismic signal (from Pakistan, a distance of 46^o) has any coherence between the elements of a single subarray. This is because the signal is dominated by frequencies below 4 Hz, a frequency above which one cannot expect signals to be coherent between such widely spaced stations. The signal to the right results from a cavity explosion in Sweden at a distance of 150 km which has very little energy below a frequency of 8 Hz (see Gibbons et al., 2002).

The only way we can hope to measure slowness and azimuth from such signals is by determining the arrival time at each of the sites to the highest possible accuracy and then fitting a best fit wavefront across the array. The large size of the array means that, for most regional phases, the time taken for a wave-front to cross the array is quite large and the capability for making a good determination of slowness and azimuth is fairly good, provided that a sufficient number of sufficiently accurate arrival times are correctly associated and that spurious arrival times are successfully removed from the inversion process.

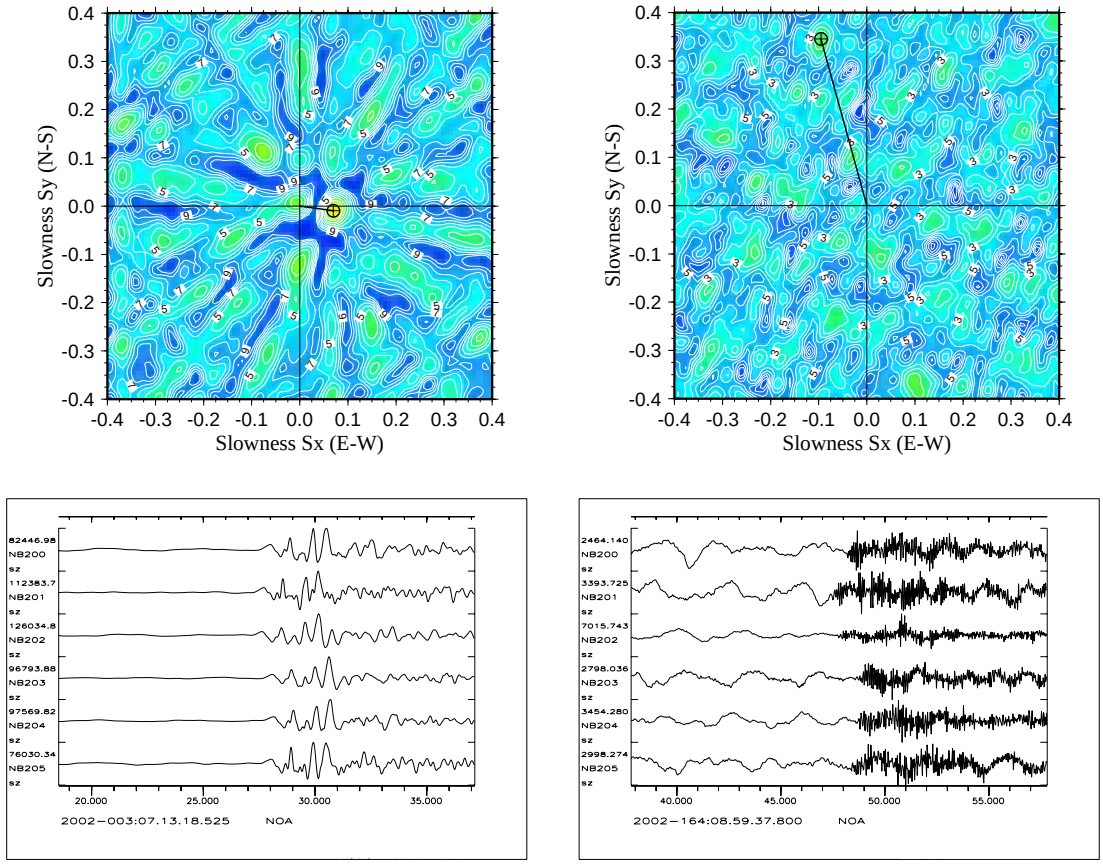

Fig. 6.4.2. Broadband fk-plots and unfiltered waveforms for a teleseismic P-arrival (Pakistan, azimuth 97^o; left) and a regional Pg phase (Sweden, azimuth 71^o; right). The fk-analysis was performed in a 3 second time window on waveforms filtered in the 1.5 - 4.0 Hz frequency band.

6.4.2 Detection and processing of regional events

Detection

It was pointed out by Ringdal et al. (1975) that by forming incoherent beams, i.e. the beams of the short term average (STA) or envelope of filtered waveforms, that high frequency signals could be detected on the NOA array with a high SNR, despite the incoherence of the actual waveforms. All short period vertical (sz) traces from each subarray are bandpass filtered in the frequency bands listed in Table 6.4.1. For a given frequency band, an STA trace is formed from each filtered signal and these STA traces are summed with time delays corresponding to the apparent velocity and azimuth values listed in Table 6.4.1.

Frequency band (Hz)	Azimuth values (degrees)	Apparent velocities (kms^{-1})
(2.0 - 5.0)	0, 45, 90, 135, 180, 225, 270, 335	3.8, 6.5, 9.0, 12.0
(3.0 - 6.0)		
(4.0 - 8.0)		
(6.0 - 12.0)		
(8.0 - 16.0)		

Table 6.4.1. Subarray beams used for the processing of regional events at the NOA array.

In the current prototype version of the Regional NOA processing system, all detections are made at subarray level. However, the system is designed such that a beam with arbitrary delays for any combination of sites could be introduced. Hence, travel times for a given phase from a specific site could be calculated and incorporated into a beam. An event occurring at that site would then be likely to result in a beam with a higher SNR than any of the single subarray beams.

Processing

Having made a detection, the frequency content of the signal must be estimated for each of the single traces which contributed to the detection; for all but the lowest frequency signals, the traces must be analysed individually. For each trace, a frequency band is calculated in which the SNR is a maximum; these calculations provide a trigger time which can be used as an initial estimate for a more accurate onset time determination, taking into account changes in both frequency and amplitude. For this, we use the autoregressive AR-AIC method (Akaike, 1974; GSE/JAPAN/40, 1992). The task is then to associate as many arrival times as possible (at a maximum of 42 sites in the NOA array) which correspond to the same phase arrival.

At the sub-array level, with inter-station distances of up to 9 km, most incoming wave-fronts can adequately be modelled as planar wave-fronts. However, over the full NOA array, the maximum distance between stations is almost 80 km, meaning that departures from planar geometry will be significant for events up to 250-300 km from the array's reference point. Although fitting a plane wave to a set of arrival times from such an event is likely to result in an azimuth and slowness which are approximately correct, the deviations from the best-fit wavefront will be systematic and large such that an imbalance in measurement (for example

should we fail to measure any satisfactory arrival times from one or more of the sub-arrays) is likely to lead to a spurious slowness determination. Almendros et al. (1999) successfully applied a circular wave-front to seismo-volcanic sources at local distances at Deception Island, Antarctica, and we will here apply this formulation to events at regional distances arriving at the NOA array.

Using the notation of Almendros et al. (1999), we assume incoming wavefronts to travel at a constant slowness, S, from an origin a distance D from the array reference point (x_0, y_0) at an azimuth A (see Fig. 6.4.3); the time taken for the wave to reach a station *k* is

$$t_k = S\sqrt{(x_k - D\sin A)^2 + (y_k - D\cos A)^2} \qquad (1)$$

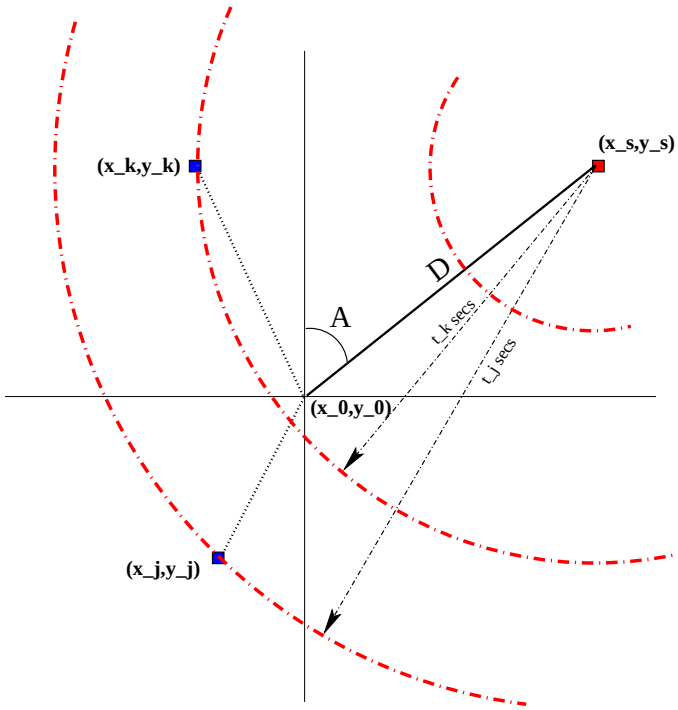

Fig. 6.4.3. The circular wave-front geometry proposed by Almendros et al. (1999).

We will have a maximum of 42 arrival times from which we must solve for the unknowns D, S, and A, along with t_0, the time at which the circular wave passes the reference point of the array. Unlike the plane wave fit, this system is non-linear and so cannot be solved by a straightforward least squares inversion. Almendros et al. (1999) used a grid search method to find the parameters best fitting the given arrival times. However, at the local distances in their study, the signals were largely coherent and the iterative process involved correlating waveforms which is not a practical solution for us. Instead, we employ a Newton-Raphson type iteration based upon the arrival times alone which minimizes the (observed - predicted) time residuals. This requires an initial estimate of the parameters, of which t_0, S, and A are available from the linear plane wave fit.

The distance D is not considered to be an important parameter in this situation for two reasons; firstly, the formulation does not take into account the curvature of the Earth which will be non-

negligible over regional distances and, secondly, a circular wave travelling at a constant velocity is a gross oversimplification of the true seismic wavefield. In many cases, where the origin of the event is several times further from the array reference point than the array aperture, the curvature of the wavefront will be insignificant compared with the uncertainties in the arrival time determinations and we will not be able to solve for D. In such cases, the circular wavefront fit returns the best fit plane wavefront. The array reference point for NOA was selected to be site NB200 (coordinates 61.03972^{o}N, 11.21475^{o}E).

Arrival times are grouped at subarray level for a given detection. This allows for some additional screening of outliers, i.e. onset time determinations which passed the SNR tests on the individual traces, but which cannot correspond to the same seismic phase as the other picks from the subarray. The most difficult task remains; we need to associate the subarray detections which correspond to the same seismic phase. The incorrect association of subarray detections is by far the most likely cause of false alarm reporting. If a slowness and azimuth determination of a genuine seismic phase is made with onset times from a subset of NOA elements, we should obtain confidence intervals in which we can anticipate arrivals from the same seismic phase at the remaining NOA instruments. Subsequent detections which do not fall within these time intervals clearly do not belong to the same event and are readily screened out. However, there are many instances where two groupings of arrival times which do not correspond to the same seismic phase are grouped together simply because they occur in the same time window. This will may return an azimuth and slowness corresponding to a non-existent seismic phase, prevent the detection of a genuine phase, or both. Such cases will be discussed later in more detail.

6.4.3 Results from circular wavefront fitting at the NOA array

To demonstrate the validity of the circular wavefront fit to regional data, we selected a series of 12 explosions performed by the Swedish military in June and July 2001 at the Mossibränden site in Älvdalen Skjutfält (coordinates 61.566^{o} N, 13.790^{o} E). Details of these events are given in Gibbons et al. (2002). The explosion site is 152.40 km from the centre of the NORES array with a receiver to source backazimuth of 51.63^{o}. The backazimuth for site NB200 of NOA is 65.85^{o} at a distance of 149.94 km. The station to source distances vary from 119 km (NC401) to 183 km (NAO04) and backazimuths vary from 51.3^{o} (NC603) to 79.0^{o} (NC205).

The Pg phase is anticipated to be the first arrival from these events at those elements of the NOA array closest to the source. In southern Norway, the Pn phase replaces Pg as the first arrival at an epicentral distance of approximately 150 to 170 km (Gundem, 1984). The more distant elements of the NOA array may therefore experience the Pn phase first, with a higher apparent velocity than Pg. Given that the arrival times used for an inversion of a best fit circular wavefront will invariably be either a first P-arrival or a first S-arrival, this case study potentially illustrates a fundamental problem; we are attempting to fit a wavefront with a constant slowness to arrival times corresponding to different seismic phases.

The waveforms recorded from a typical one of these events at NOA are displayed in Fig. 6.4.4. These events were all detected with a high SNR and satisfactory automatic P-arrival times were calculated for most traces for all events. The S-phase picks were predictably poorer with many determinations being discarded as the result of low signal to noise ratio. The AR-AIC method works best for arrivals where the signal and preceding noise exhibit a large contrast in both amplitude and frequency content. In order to obtain an optimal SNR, most such traces

have to be filtered in quite a narrow frequency band (typically between 2.0 and 5.0 Hz) and the contrast in the autoregressive models is consequently small.

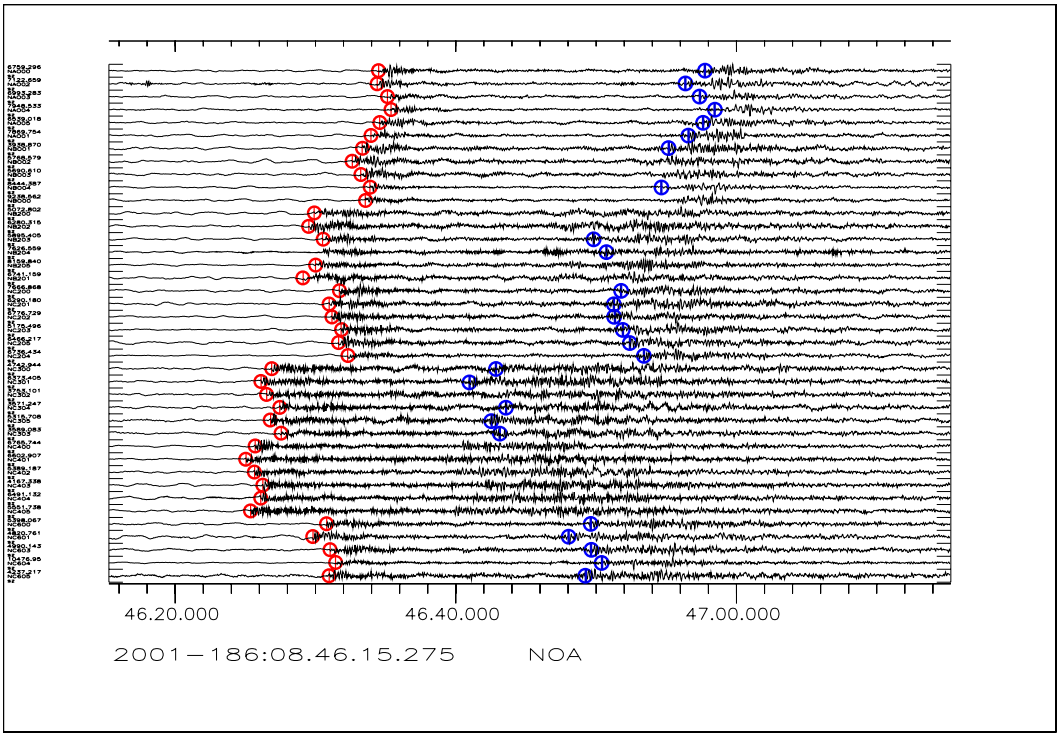

Fig. 6.4.4. Unfiltered waveform data from one of the Mossibränden explosions with the automatically calculated arrival times for P (red symbols) and S (blue symbols). An S-onset time is missing from many of the traces; this indicates that the onset picker failed, either due to a low SNR or a bad value of the Akaike Information Criterion (AIC).

Table 6.4.2 gives the azimuth values obtained for the P-arrivals from this series of events as determined by the NORES array using standard broadband fk-analysis, and by the NOA array where a best fit circular wavefront is fitted to automatically determined onset times. The azimuths determined by fk-analysis in a fixed frequency band (NORES) have a small standard deviation but a large systematic departure from the geographical backazimuth. The offset in azimuth is a function of the frequency band used for the analysis, reflecting the complicated form of the seismic wavefield resulting from the heterogeneous underlying velocity structure (see Kværna and Doornbos, 1991). The azimuths reported by the automatic event processor for NORES show a very large standard deviation but mean and median values which lie quite close to the actual values. This is due to the fact that the fk-analysis is performed in a frequency band which is not fixed but determined automatically to optimize the SNR. Fluctuations in SNR, for instance due to different levels of background noise, may lead to small differences in the selected frequency band and consequently large differences in azimuth as documented by Kværna and Doornbos (1991).

The azimuth values from the circular wavefront fits have both a small systematic offset and a low standard deviation. The large area covered by the NOA array means that many scattering effects and local wavefield properties are averaged out between the widely spaced sensors. The azimuth value returned is only a function of the measured onset times which are relatively

insensitive to variations in the background noise. Although the distance parameter, *D*, is not a reliable indicator of epicentral distance in general, the closeness of these *D* values to the geographical distance indicate that there is much validity in the circular approximation to the shape of the wavefront for these events.

Origin time	Azimuth deviation from NORES from fk-analysis in a fixed frequency band (2.0 - 5.0 Hz)	Azimuth deviation from NORES automatic processing	Azimuth deviation for circular wavefront - NOA	Distance, *D*, determined from circular wavefront - NOA
2001-176:13.46.17.89	-9.65 (41.98)	-9.03 (42.6)	-0.44 (65.41)	148.07
2001-177:07.15.30.24	-9.64 (41.99)	-8.93 (42.7)	-0.72 (65.13)	156.99
2001-177:13.00.10.52	-9.38 (42.25)	-9.63 (42.0)	-0.47 (65.38)	151.13
2001-178:09.16.05.37	-9.20 (42.43)	7.77 (59.4)	-0.57 (65.28)	159.30
2001-178:13.40.12.41	-8.85 (42.78)	6.87 (58.5)	-0.51 (65.34)	171.23
2001-179:09.40.55.57	-9.84 (41.79)	2.97 (54.6)	-0.65 (65.20)	157.08
2001-179:13.50.31.67	-8.35 (43.28)	4.47 (56.1)	-0.60 (65.25)	163.52
2001-183:11.36.00.64	-8.59 (43.04)	3.17 (54.8)	-0.78 (65.07)	151.42
2001-184:07.31.03.74	-9.26 (42.37)	-9.13 (42.5)	-0.56 (65.29)	153.24
2001-184:13.01.01.21	-9.95 (41.68)	-8.03 (43.6)	-0.67 (65.18)	153.07
2001-185:09.36.06.49	-9.74 (41.89)	3.57 (55.2)	-0.71 (65.14)	158.69
2001-186:08.46.05.59	-8.94 (42.69)	7.17 (58.8)	-0.56 (65.29)	150.53
Standard deviation	0.513	7.42	0.105	6.48
Mean value	-9.28 (42.35)	-0.73 (50.9)	-0.603 (65.246)	156.2
Median value	-9.32 (42.31)	3.07 (54.7)	-0.585 (65.265)	155.1

Table 6.4.2. Azimuth values for the 12 Mossibränden explosions in June and July 2001 based upon the P-arrival. Azimuth deviation refers to the difference between the measured and known geographical azimuth values; the measured azimuths are given in parentheses. The actual azimuths are 51.63^{o} (NORES) and 65.85^{o} (NB200, NOA) and the distance from NB200 to the explosion site is 150 km. The corresponding apparent velocity values are given in Table 6.4.4.

The corresponding azimuth values for the S-phases are displayed in Table 6.4.3. The azimuth values obtained by the circular wavefront fit have a slightly larger offset and standard deviation than they did for the P-arrivals but, although having a higher standard deviation than the fixed frequency band fk-analysis results from NORES, still give quite accurate and consistent determinations. One crucial observation is that in most cases we failed to solve for the distance, *D*,

such that most of these determinations are actually plane wave fits. Even on the occasions when a value of *D* was returned, it was generally far larger than any realistic value and so, in effect, the circular wavefront was a plane approximation.

Origin time	Azimuth deviation from NORES from fk-analysis in a fixed frequency band (2.0 - 5.0 Hz)	Azimuth deviation from NORES automatic processing	Azimuth deviation for circular wavefront - NOA	Distance, D, determined from circular wavefront - NOA
2001-176:13.46.17.89	8.92 (60.55)	11.2 (62.9)	3.32 (69.17)	-
2001-177:07.15.30.24	7.62 (59.25)	8.4 (60.1)	2.05 (67.90)	-
2001-177:13.00.10.52	8.62 (60.25)	7.6 (59.3)	2.50 (68.35)	224.8
2001-178:09.16.05.37	8.29 (59.92)	10.4 (62.1)	3.81 (69.66)	-
2001-178:13.40.12.41	7.29 (58.92)	8.0 (59.7)	-0.99 (64.86)	318.4
2001-179:09.40.55.57	8.24 (59.87)	-0.7 (50.9)	3.27 (69.12)	-
2001-179:13.50.31.67	7.33 (58.96)	10.1 (61.8)	3.21 (69.06)	202.5
2001-183:11.36.00.64	8.05 (59.68)	-0.4 (51.2)	2.18 (68.03)	-
2001-184:07.31.03.74	7.94 (59.57)	10.2 (61.9)	3.08 (68.93)	-
2001-184:13.01.01.21	6.83 (58.46)	10.6 (62.3)	1.06 (66.91)	299.6
2001-185:09.36.06.49	7.36 (58.99)	9.3 (61.0)	3.15 (69.00)	-
2001-186:08.46.05.59	7.99 (59.62)	9.2 (60.9)	2.02 (67.87)	175.69
Standard deviation	0.607	4.10	1.31	-
Mean value	7.87 (59.50)	7.87 (59.51)	2.39 (68.24)	-
Median value	7.97 (59.60)	9.32 (60.95)	2.79 (68.64)	-

Table 6.4.3. Azimuth values based upon the S-arrivals for the 12 Mossibränden events (c.f. Table 6.4.2). The absence of a *D* value indicates that this parameter could not be solved for in the circular wavefront inversion and the azimuth and slowness obtained correspond to that of a plane wave. The corresponding apparent velocity values are given in Table 6.4.4.

Finally, Table 6.4.4 lists the apparent velocities obtained by the same three calculations as provided the azimuth values in Tables 6.4.2 and 6.4.3. The circular wavefront fit for the NOA array gives very consistent values around 6.17 kms^{-1} for the apparent velocity of the P-arrival; slightly lower than those obtained by the fk-analysis at the NORES array. For the S-arrival, with the correspondingly poorer onset time estimations, the slowness determinations from NORES are more stable than the NOA circular wavefront fits. NORES and the NB200 site are

essentially equidistant from the source site and so the apparent velocities should be directly comparable.

Origin time (abbreviated)	Apparent velocity: P-arrival			Apparent velocity: S-arrival		
	Fixed band fk-analysis: NORES	Automatic processing: NORES	Circular wave front fit: NOA	Fixed band fk-analysis: NORES	Automatic processing: NORES	Circular wave front fit: NOA
2001-176	6.68	6.3	6.20	3.60	3.6	3.33
2001-177a	6.73	6.3	6.15	3.61	3.3	3.23
2001-177b	6.53	6.3	6.18	3.57	3.4	3.43
2001-178a	6.62	6.6	6.16	3.54	3.6	3.34
2001-178b	6.60	6.4	6.14	3.53	3.5	2.99
2001-179a	6.61	6.7	6.18	3.57	3.3	3.44
2001-179b	6.48	6.6	6.17	3.51	3.8	3.30
2001-183	6.54	6.6	6.17	3.55	3.1	3.26
2001-184a	6.55	6.4	6.17	3.55	3.6	3.42
2001-184b	6.60	6.3	6.19	3.54	3.6	3.35
2001-185	6.68	6.5	6.17	3.56	3.5	3.27
2001-186	6.65	6.5	6.18	3.65	3.6	3.21
Standard deviation	0.0724	0.144	0.0164	0.0387	0.188	0.123
Mean value	6.61	6.46	6.17	3.57	3.49	3.30
Median value	6.61	6.45	6.17	3.56	3.55	3.32

Table 6.4.4. Apparent velocity for P and S arrivals at NORES and NOA for the events listed in Tables (6.4.2) and (6.4.3).

6.4.4 The detection and location capabilities of the NOA array at regional distances

Automatic detections from the prototype regional NOA processing system have been included in a test version of the GBF process. Fig. 6.4.5 shows the trial locations of events, from a test period of 90 days in 2003 (after NORES data became unavailable), which included at least two defining phases from the NOA array. The green symbols correspond to events which were also detected by other arrays, especially the Hagfors array in Sweden. Many of these events were

also located by GBF without the NOA phases, although the additional arrival times and azimuth information provide a useful additional constraint on epicenter location.

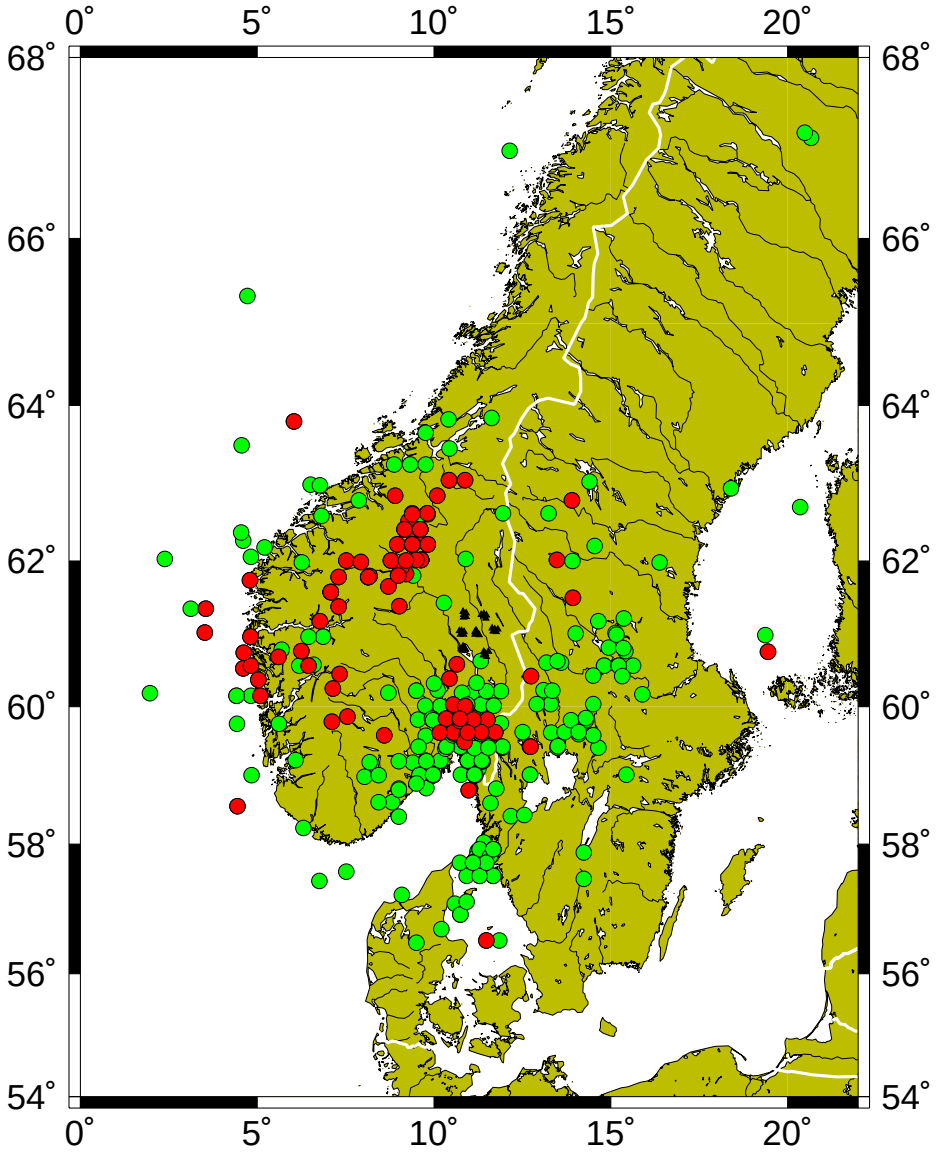

Fig. 6.4.5. Events located by the GBF system over a trial period from 2003-001 to 2003-090 which include at least two phases from the Regional NOA process. Red symbols indicate that the events were only located by phases detected using NOA; green symbols indicate that at least one phase from another array was used in addition.

Events displayed here which are only detected by NOA and which are, for example, closer to the HFS array than to NOA are very likely to be false associations, as is the red symbol in the Gulf of Bothnia in Fig. 6.4.5. Most of the symbols in Sweden correspond to events for which the directional and time observations from NOA are consistent with those from HFS. Most of the events only detected by NOA are in the range 80 - 200 km from the array and are generally associated with high frequency signals. These are ideally suited to processing with this system. Although the signals are weak, their high frequency content allows for good onset-time determinations by the AR-AIC process; the low energy content at lower frequencies mean that signal coherency is often poor, even for regional arrays such as Hagfors. The large cluster of

events in central Norway (Oppland) are presumed to be industrial due to the patterns of occurrence. They are probably far more clustered than indicated in Fig. 6.4.5; azimuths from the P-arrivals fall into very narrow ranges, but the S-phases have far fewer, and poorer, onset time determinations and consequently are attributed azimuth values that are poorly constrained.

If we increase the scope of Fig. 6.4.5 to include GBF locations with only a single defining phase from NOA then we obtain many events much further away than those shown, which generally occur within approximately 350 km of the array. There are however, many more false alarms. Slowness and azimuth values have been determined from a great many P-arrivals with very small time residuals. However, in the absence of a good determination of a secondary phase, these events can not be located unless they are successfully associated with phases detected at other arrays. In its current form, there are very few events for which the process has managed to make satisfactory azimuth and slowness determinations for all of the Pn, Sn, and Lg phases.

6.4.5 Discussion and further work

We have developed a system by which seismic phases from regional events can be identified using the NOA array. The system works by calculating the arrival times of phases at each of the short period vertical instruments in the array and by fitting a wavefront to those arrival times. The circular wavefront formulation of Almendros et al. (1999) was found to give very robust and realistic estimates of slowness and azimuth of phases at near-regional distances, an iterative process being employed to find the parameters which minimize time residuals. This iterative method could robustly be applied to all arriving wavefronts because the limiting case of the circular wavefront is a plane wavefront.

The system has been quite successful at locating events within approximately 350 km of the array and many events which have not been detected by the GBF system since the loss of the NORES array can now be included. The NOA array can also provide a useful constraint on events which otherwise would only be detected by the Hagfors array.

The fundamental disadvantage of using NOA is that the signals of interest are not coherent over the array and we are thus limited to examining each trace individually. This is to say that once a detection has been made by incoherent beamforming, the elements of NOA act merely as a network and not an array. Only when we are able to determine with confidence a phase arrival time on a single trace is that data useful in identifying a phase. This somewhat defeats the purpose of seismic arrays which is to improve the information which can be obtained from signals by combining data from different sites in such a way that the form of the signal is amplified and the noise reduced. Nuances of seismic signals, especially the arrival of coda phases, which are readily available from regional arrays (Mykkeltveit and Bungum, 1984), will never be discernible using the methods outlined here and a wealth of information regarding the seismic wavefield will be lost until a replacement for NORES is obtained. The best we can hope to do with the method outlined here is to obtain an arrival time, slowness and azimuth for first P-arrivals and a secondary phase; it is very seldom that more than one secondary phase can be correctly identified by the picking of arrival times on traces from such widely spaced instruments.

The principal reason for failure of the current system is an incorrect association of detections and corresponding arrival times at subarray level. For incoherent regional signals, it is gener-

ally necessary to associate detections from several subarrays to make a worthwhile estimate of the slowness and azimuth of an incoming phase. With 6 instruments in a subarray, although it is certainly possible to invert these arrival times for the parameters of a plane wavefront, the uncertainties associated with the slowness and azimuth can be large and an automatically picked arrival time needs only an error of a few samples to have a large effect on the predicted wavefront. Many single subarray determinations for P-arrivals are actually quite good due to the low error associated with the time picks. For S-arrivals, however, the error associated with each pick is usually comparable with the time delay between the stations. On the other hand, if the onset times from several subarrays are combined, the errors on individual picks become insignificant compared with the total time delays. This is beautifully illustrated in Fig. 6.4.4 where the S-arrival times from the whole array result in an azimuth determination within 2^{o} of the geographical value and an apparent velocity with an error less than 10%.

It takes approximately 20 seconds for a regional S-phase to cross the NOA array. Any unrelated phase arriving in this period can lead to an erroneous determination which, without a sophisticated checking mechanism, will also result in a missed determination of a genuine regional phase. An unassociated P-arrival at one subarray, combined with an S-arrival at another subarray, can result in a plausible wavefront with a far higher apparent velocity: a spurious teleseismic phase. Similarly, two detections from different segments of the coda of a teleseismic signal can combine such that a best fit wavefront gives the slowness and azimuth of a regional phase. Processing regional events on a small aperture array or teleseismic events on a large aperture array can largely be done serially; i.e. without the need to examine the history of the time series. To minimize the occurrence of spurious regional associations on the NOA array, it is probably necessary to examine a long time segment with potentially many detections on each subarray and try to deduce the most likely phase combinations. This is non-trivial.

The remaining challenges to the process are to improve the determination of onset times for secondary phases (the absence of secondary phases is the primary reason that so many events with well determined P-arrivals remain unlocated) and to improve the detection and processing of events at far-regional distances. The key to the first issue is almost certainly the use of the rotated horizontal components of the 3-component broadband instruments, of which one is located in each subarray. The key to the second issue is probably the use of detecting beams which cover more than one subarray: possibly with the additional use of the 3-component instruments. However, to prevent a prohibitively large number of beams, an optimal combination of frequency bands and time-delays must be investigated for the events of interest. Ultimately, we must accept the limitations of such a large aperture array and accept that if we have neither sufficient signal coherence (at least at subarray level) or a signal which is sufficiently strong that it can be analysed on a single component (be it short period vertical or rotated), then we have exceeded the capability of NOA and need a regional array solution.

Steven J. Gibbons
Tormod Kværna
Frode Ringdal

References

Akaike, H. (1974). Markovian representation of stochastic processes and its application to the analysis of autoregressive moving average processes. Ann. Inst. Stat. Math. **26**, 363-387.appearance

Almendros, J., Ibáñez J. M., Alguacil, G, and Pezzo, E. D. (1999). Array analysis using circular-wave-front geometry: an application to locate the nearby seismo-volcanic source. Geophys. J. Int., **136**, 159-170.

Bungum, H. and Husebye, E. S. (1974). Analysis of the operational capabilities for detection and location of seismic events at NORSAR, Bull. Seism. Soc. Am. **64**, 637-656.

Bungum, H., Husebye, E. S., and Ringdal, F. (1971). The NORSAR array and preliminary results of data analysis. Geophys. J. R. astr. Soc. **25**, 115-126.

Gibbons, S. J., Lindholm, C., Kværna, T., and Ringdal, F. (2002). Analysis of cavity-decoupled chemical explosions. In *Semiannual Technical Summary*, 1 January - 30 June 2002. NORSAR Sci. Rep. 2-2002, Norway.

GSE/JAPAN/40. (1992) A Fully Automated Method for Determining the Arrival Times of Seismic Waves and its Application to an on-line Processing System. In *Proceedings, 34th GSE session, Geneva, Switzerland. GSE/RF/62, G.S.E.*

Gundem, M. B. (1984). 2-D Seismic Synthesis of the Oslo Graben. Cand. scient. thesis. University of Oslo.

Kværna, T. and Doornbos, D. J. (1991). Scattering of Regional Pn by Moho Topography. Geophys. Res. Lett., **18(7)**, 1273-1276.

Kværna, T. and Ringdal, F. (1996). Generalized beamforming, phase association and threshold monitoring using a global seismic network. In *Monitoring a Comprehensive Test Ban Treaty* (eds. E. S. Husebye and A. M. Dainty), Kluwer Academic Publishers, 447-466.

Mykkeltveit, S. and Bungum, H. (1984). Processing of Regional Seismic Events Using Data from Small-Aperture Arrays. Bull. Seism. Soc. Am. **74**, 2313-2333.

Mykkeltveit, S. and Ringdal, F. (1981). Phase identification and event location at regional distance using small-aperture array data, In *Identification of seismic sources - Earthquake or underground explosions* (eds. Husebye, E. S. and Mykkeltveit, S.) pp. 467-481.

Mykkeltveit, S., Ringdal, F., Kværna, T., and Alewine, R. W. (1990). Application of Regional Arrays in Seismic Verification Research. Bull. Seism. Soc. Am. **80**, 1777-1800.

Ringdal, F., Husebye, E. H. and Dahle, A. (1975). P-Wave Envelope Representation in Event Detection Using Array Data, In *Exploitation of Seismograph Networks* (ed. K. G. Beauchamp), Noordhoff - Leiden, NATO Advanced Study Institutes Series, Series E: Applied Sciences - No. 11.

Ringdal, F. and Husebye, E. H. (1982). Application of arrays in the detection, location, and identification of seismic events. Bull. Seism. Soc. Am., **72**, S201--S224.

Ringdal, F. and Kværna, T. (1989). A multi-channel processing approach to real time network detection, phase association, and threshold monitoring. Bull. Seism. Soc. Am., **79**, 1927-1940.